Chapter 10

Operation of Plug-In Electric Vehicles for Voltage Balancing in Unbalanced Microgrids

Guido Carpinelli, Fabio Mottola, Daniela Proto and Angela Russo

Additional information is available at the end of the chapter

http://dx.doi.org/10.5772/intechopen.68894

Abstract

The widespread use of distributed energy resources in the future electric distribution systems represents both a challenge and an opportunity for all the Smart Grid operators. Among these resources, plug-in electric vehicles are expected to play a significant role not only for the economic and environmental benefits they involve but also for the ancillary services they can provide to the supplying grid. This chapter deals with real-time operation of unbalanced microgrids including plug-in electric vehicles. The operation is achieved by means of an optimal control strategy aimed at minimizing the costs sustained for the energy provision while meeting various technical constraints. Among the technical constraints, the optimal control allows guaranteeing the satisfaction of power quality requirements such as the containment of slow voltage variations and the unbalance factors. Case studies are investigated in order to show the feasibility and the effectiveness of the proposed approach.

Keywords: microgrids, slow voltage variations, unbalances, optimal control strategy, plug-in vehicles

1. Introduction

Smart grids (SGs) are playing a vital role in the future of power systems mainly due to their potential to minimize costs and environmental impacts while maximizing reliability, power quality (PQ), resilience, and stability. These goals can be attained by means of a proper exploitation of the SG's distributed energy resources (DERs). However, the integration of DERs (i.e., generation units, controllable loads, and energy storage-based devices) is a challenging task in the view of the optimal planning and operation of the SGs. Thus, new research contributions aimed to guarantee the DER correct behavior are of high interest for all the

involved operators (from System Operators to Electric Utilities and Energy Traders, Independent Power Producers and Consumers). Among the energy storage-based devices, plug-in electric vehicles (PEVs) are achieving particular attention in the relevant literature. PEVs, in fact, are expected to have a wide diffusion in the next future especially due to the current attention paid worldwide to the reduction of greenhouse gas emissions mainly caused by the use of internal combustion engines. However, PEVs require to charge from the power grid, then their massive spread could pose critical issues. The charge of a large number of PEVs is a huge load demand that the grid is called to face and a number of problems can occur in terms of PQ degradation, instability of electrical networks, and degradation of operation efficiency [1]. On the other hand, PEVs connection to the grid could represent also an opportunity due to the presence of on-board batteries that could have an important role in grid operation. The electrical energy storage devices, in fact, are a particular typology of loads that are expected to be key components in modern power systems. When opportunely coordinated, these devices can become distributed resources for the grid so providing benefits rather than criticisms to it. The benefits achievable by their use are mainly related to voltage support, price arbitrage, PQ, reliability improvement, reduction of the cost for energy provision, and renewable energy fostering. In order to gain these benefits, the storage systems need specific charge/discharge control strategies able to account for the requirements of the storage itself and of the grid they are connected to, in addition to adequate communication infrastructures. In particular, when the storage systems are included in a microgrid (μG), the control strategies should guarantee the correct operation of the whole μG taking into account also the presence of other controllable sources, such as DG units and dispatchable loads. In these cases, the adopted control tasks should take into account also the possibility of load shedding or generation curtailment in case of increased demand or generation, respectively.

A proper PEV control strategy would take into account targets such as cost minimization and PQ improvement.

Regarding the first target, in the frame of demand response paradigms, PEVs have a great potential. More specifically, in the case of dynamic pricing schemes, an appropriate control of PEVs charging would allow reducing costs by shifting the peak load in response to changes in the price of electricity over time. Different time-based rate programs are available: time-of-use (TOU) pricing refers to different prices applying to determined periods of the day (block of hours of the day). In these periods, the tariff is constant. Real-time pricing (RTP) is characterized by pricing rates typically applying on an hourly basis. Variable peak pricing (VPP) is a hybrid of time-of-use and real-time pricing not only with different periods of the day for pricing but also with a price for the on-peak period that depends on market conditions. With the critical peak pricing (CPP), utilities identify critical events during a specified time period when the price for electricity may substantially increase (e.g., very hot hours in a summer afternoon). Finally, critical peak rebate (CPR) is a pricing structure similar to the CPP that allows customers to be paid for cutting back on electricity during critical events relative to the amount they normally use [2]. In this variegated pricing scenario, the optimal operation of PEVs allows substantial reduction of the operation costs for the μG that could optimize the expense for the energy provision. Of course, an optimized control should be performed by taking into account the preferences and the comfort levels required by the vehicle owners.

Regarding the PQ improvement target, several benefits can be achieved by a proper control of the PEV charging. In the case of low voltage (LV) μGs, typically characterized by the presence of unbalances, the benefits PEVs can provide are even more significant. LV μGs, in fact, are characterized by significant unbalances due to their structure, to the presence of single-phase loads and renewable generation units (i.e., single-phase photovoltaic systems). For this reason, voltage unbalances can be excessive and represent a burdensome PQ issue [3]. Consequences of unbalances in LV μGs can be the increase of losses and heating effects affecting power electronic converters and induction motors [4], overloading of distribution feeders and transformers [5], excessive mechanical stress and noise due to a double system frequency in the synchronous generators equipping microgeneration units [6].

This chapter is framed in this multifaceted scenario of μG real-time operation and deals with advanced strategies for the control of μG's distributed energy sources (DERs) aimed at minimizing operation costs and at ensuring an optimal grid and storage systems operation with reference to various technical constraints. More specifically, the DERs to be optimally controlled in the considered μG are: the batteries on board the electric PEVs connected to the grid for charging and the DG units connected to the grid through power converters. The optimal operation of μG refers to the cost minimization under real-time pricing while grid constraints on bus voltages and line currents are satisfied. Among the voltage constraints, a maximum allowed voltage unbalance factor is imposed on the basis of the current standards [7]. Specific requirements for the storages (e.g., a vehicle's battery has to be fully charged at a specified departure time) are also guaranteed.

The proposed control strategy refers to real-time operation and helps the μG's operator better control the operational processes and plan appropriate energy market bidding, due to the most proficient use of electrical storage systems. It is formulated as a multi-period non-linear constrained optimization problem (OP) which aims at minimizing the energy costs for the whole μG while satisfying technical constraints related to the correct operation of the components and of the grid as well as to the needs of the vehicle owners.

The technical strength of the proposed operation strategy is related to the proper control of DERs which allows

- minimizing the costs for energy provision;
- complying with the standard limits for the slow voltage variations and voltage unbalances, which are among the most severe PQ phenomena in LV μGs;
- mitigating the impact of very large loads, by containing line currents and bus voltages within admissible ranges; and
- increasing grid capability in terms of power injection from distributed energy sources.

This chapter is structured as follows. The state of the art of the PEV charging devices and the challenges and benefits related to their inclusion in μGs are described in Section 2. Section 3 shows the analytical formulation of the proposed control strategy. The results of numerical applications are reported in Section 4. Finally, Section 5 draws conclusions and opens problems for future research.

2. Plug-in vehicles in the frame of low voltage microgrids: State of the art

The relevant literature on plug-in electric vehicles is very wide and rich. In this section, review papers are mentioned to a large extent and, in some cases, research papers are shown on particular topics.

2.1. Classification of charging systems

One of the key elements of a successful electric vehicle diffusion is the charging equipment. Some common features are required for the electric vehicle charger (EVC), for example, battery performance, high reliability of the charger, high power efficiency, and minimum impact on the PQ [8]. In addition, since a large-scale diffusion of PEVs can also pose new challenges for the power system operators (e.g., congestions, voltage profiles, etc.), the "smart" charging solutions may transform PEVs in a resource for the system [9–11].

With specific reference to PEVs, in Ref. [1], the battery charging schemes are classified as follows: uncontrolled, indirectly controlled, smart, and bidirectional. In the uncontrolled charging, the vehicle immediately begins recharging as soon as it is connected to the grid. Indirectly controlled, smart, and bidirectional charging schemes are used to control energy prices; in the smart charging schemes, the battery charging is subject to some measure of intelligent control by the utility or system operator.

Regarding the charger device, an AC/DC converter is required since the batteries charge by absorbing DC power. The main function of this converter is to rectify the AC power from the electrical grid. Chargers can be installed on board and off board of the vehicles. On-board charger is often designed in small size to reduce the weight burden for PEV. Off-board chargers are particularly convenient in fast charging service [12].

Different charging methods can be implemented. Ref. [12] classifies the charging methods as constant current, constant voltage, constant power, taper charging, trickle charging, advanced charging that involves combination of the above methods, pulse-charging and negative pulse-charging.

2.2. Adverse effects and services provided by plug-in electric vehicles

PEVs can be operated in two configurations when connected to the electric grid:

- Grid-to-vehicle, usually referred to as V1G (also G2V); and
- Vehicle-to-grid, usually referred to as V2G.

In the first configuration, the flow of the electric power is uni-directional, that is, the electric power flows from the grid to the PEVs. In the second configuration, the flow of the electric power is bi-directional, that is, the PEV can absorb electric power from the grid and inject electric power to the grid. In this case, PEVs can be assimilated to a distributed energy resource (distributed generator or storage system).

A large number of studies indicates some adverse effects of PEVs on electric distribution systems (for instance, see the review Ref. [13]). Among them, we can mention voltage instability, increased

peak demand, PQ problems (e.g., voltage profile, voltage unbalance, harmonics, etc.), increased system energy losses, transformer heating, and overloading [12–14]. It should be noted that most of them occur when the charging of vehicles is uncoordinated.

In spite of the impact on the distribution systems, PEVs are considered valuable resources for the electric power grids because they can provide a large number of services to the local distribution system and also to the power system. When V1G configuration is adopted, the charging method assumes an important role. For instance, shifting the charging to off-peak periods can be exploited to better integrate a large diffusion of PEVs into the electricity grid. Another contribution [15] proposes an integration of PEVs able to improve the PQ levels of the distribution system. An autonomous control of PEVs charging systems (in V1G configuration) is proposed in order to reduce voltage unbalances in a distribution network, in which local voltage measurements drive the modulation of the charging current.

However, the most promising configuration is the V2G.[1] V2G power is an interesting concept that was first proposed in Ref. [16]. Operating in V2G mode, a PEV can provide services to the grid when it is parked. Considering that PEVs are parked much of the time (e.g., Ref. [17] estimates a parking time equal to 96% of the time), the contribution can be important. Typical services that PEVs are able to provide in the V2G operating mode are [12, 18]:

- baseload power and peak power provision; and
- ancillary services (frequency control, load balance, and spinning reserve services).

Other services provided in V2G mode [18, 13, 9] are reactive power support (for instance, Ref. [19] proposes a coupled energy and reactive power market considering the contribution of PEVs), power leveling (i.e., valley filling and peak shaving), and PQ improvement (for instance, harmonic filtering). In addition, in the presence of high penetration of intermittent renewable power generation, the V2G mode can be exploited to use PEVs as storage systems, backup systems, and to balance power fluctuations.

As a consequence of V2G diffusion, an increase of stability and reliability of the distribution system and a reduction of distribution costs are expected [20].

2.3. Plug-in electric vehicles modeling in μGs

μG operation is significantly affected by the wide diffusion of PEVs, in both configuration V1G and V2G. In the relevant literature, a lot of scientific contributions inquire into the possible exploitation of PEVs to provide numerous services at μG level and to strengthen the operation of a μG.

An early contribution [21] analyzes a large exploitation of PEV batteries in islanded operated μGs and proposes several control strategies to improve μG islanding.

One issue considered in the relevant literature is the day-ahead scheduling when PEVs are present in the μGs. Many contributions are available [22–29]. The proposed models may take

[1] A thorough comparison between V1G and V2G configurations is provided in Ref. [13].

into account the uncertainties of the problem variables, characteristics of different intermittent energy resources, and different optimization objectives. The integration of intermittent generation and PEVs into scheduling problems is taken into account in [23, 24, 26–29].

A two-stage energy scheduling for a μG with renewable generation is proposed in Ref. [23] and the impact of PEVs on the energy scheduling is evaluated considering different charging schemes. A two-stage framework for a μG, including PEVs and solar energy generation, is proposed also in Ref. [26]; at the first stage, a stochastic energy schedule problem is formulated for the next 24-h operation; then at the second stage, a predictive online charging control method is implemented to account for uncertainties. Also in Ref. [28], the uncertainty of the load demand and of PEVs along with the intermittency of the renewable energy resources are taken into account in the μG energy scheduling. In particular, peculiarities of wind generation and coordination among wind power plants and PEVs are considered in Refs. [22, 30, 31]. In Ref. [22], a solution of the coordinated wind and PEV (in V2G configuration) energy dispatch problem in a stochastic framework is proposed; uncertainties of wind power and of PEV driving patterns are taken into consideration. In Ref. [30], the problem of power balance in a μG including PEVs and wind turbines is addressed and a hierarchical stochastic control scheme for the coordination of PEV charging and wind power is proposed.

The presence of responsive loads together with PEVs and intermittent generation is considered in Ref. [27], where the PEVs are used to reduce peak power and modify load curves.

In Ref. [25], a regional energy management strategy based on the use of PEVs and battery swapping stations whose charging is coordinated by a price-incentive model is proposed.

The optimization models formulated for the μG energy scheduling take into account several objectives, such as the minimization of the expected total operation costs [28], the minimization of the total cost of PEVs and maximization of the profit of battery swapping stations [25], the minimization of the total cost of the network including the cost of power supply for loads and PEVs as well as the cost of energy not supplied [29].

Particular case studies are presented in Refs. [32–34]. Ref. [32] proposes to jointly control the electricity consumption of home appliances and PEVs in a μG context; in Ref. [33], an office building μG, and in Ref. [34], a commercial μG are considered.

Further topics related to the presence of PEVs in μGs are considered in the relevant literature. Refs. [35, 36] address the problem of the unit commitment for μGs including also PEVs. In particular, Ref. [36] proposes a probabilistic model able to account for the uncertainties on wind power generation, loads, and PEVs operation.

V2G strategies are developed to allow PEVs to contribute to congestion management to help maintain a secure state of the grid supporting the system in critical conditions [37]. The presence of PEVs can also be used to actively participate in μG service restoration, as shown in Ref. [38]. In addition, PEVs have been demonstrated to be able to support the system also in smoothing frequency fluctuations due to insufficient load frequency control capacity. In Ref. [39], the power control of PEVs in V2G configuration is applied to compensate for the inadequate load frequency control capacity and to improve the frequency stability of μGs, especially

in island operation mode. Ref. [40] proposes a new controller able to take instantaneous power available from the fleet of PEVs in order to provide a frequency support service.

Finally, a day-ahead scheduling strategy is proposed in Ref. [3] which refers to unbalanced μGs including in addition to PEVs, other distributed resources. The operation strategy is based on a multi-objective approach, whose objective functions refer to cost minimization, PQ improvements, and energy savings.

3. Plug-in vehicles in the frame of low voltage microgrids: The proposed optimal operation strategy

SGs need to optimally operate its DERs. PEVs are particular types of DERs whose benefits can be achieved by adopting appropriate charge/discharge control strategies able to account for the requirements of the on-board storage units and of the grid they are connected to. These control strategies should take into account also the presence of other DERs and should guarantee the correct operation of the whole μG during its operation.

In this section, we formulate a control strategy based on the solution of a multi-period, nonlinear, constrained OP which aims at minimizing the energy costs for the whole μG while satisfying technical constraints related to the correct operation of the components and of the grid as well as to the needs of the vehicle owners. In particular, the technical constraints include limits on some power quality disturbances such as slow voltage variations and unbalances.

The strategy is applied to a three-phase LV μG that includes loads and distributed resources, such as DG units and batteries on board PEVs, and is connected to the MV distribution grid through an MV/LV transformer.

The loads of the μG are supposed to be non-responsive, single-phase and three-phase loads.

The DG units are assumed non-dispatchable, single-phase PV systems which are the most extensively used type of DG units in LV systems. The connection to the distribution network of the PV units through power converters allows the control of their reactive power.

The PEVs' batteries are connected to the μG using EVCs which consist of single-phase devices connected to the grid through power converters that allow the control of active power and reactive power in both charging and discharging stages.

The proposed control strategy is used to evaluate the reference signals for the converters which connect the DERs to the grid. To obtain the above signals for the kth control interval, the nonlinear, constrained OP: (i) is formulated over a time horizon Ω_k, composed of elementary time intervals, each of duration Δt, and (ii) is solved within one elementary time interval ahead the considered control interval (e.g., the control signals for the kth elementary time interval are obtained within the (k-1)th elementary time interval).

More specifically, the dispatching of the DERs must guarantee the desired energy level to be stored in all of the connected PEVs at their departure time; thus, the procedure for the kth

control interval takes into account all of the time intervals included within the longest among the plug-in times of the connected vehicles (time horizon Ω_k). Based on this consideration, the time horizon Ω_k to be considered will change along with the arrivals of PEVs, and, at each new arrival, it has to be properly defined once more. To explain how to select the adequate time horizon Ω_k for the kth control interval, let us refer to the example shown in **Figure 1**, in which the time is discretized in time intervals of duration Δt, as mentioned above. In **Figure 1**, N_{EV} is the total number of EVCs in the μG.

In the figure, for each EVC, the time intervals between the arrival and the departure of the vehicle are highlighted. For instance, the vehicle charged at the *ith* bus is already connected at the kth time interval and its departure is scheduled at the end of the $(k+n_{k,i})$th time interval. The set of time intervals $\{k,\ldots, k+n_{k,i}\}$ is referred to as $\omega_{k,i}$. The time horizon of the optimization has to account for all the vehicles connected at the kth control interval. Generally speaking, since the control procedure would account for the desired energy stored into the batteries of all of the plugged vehicles, the time horizon of the optimization at the kth control interval is:

$$\Omega_k = \{k, \ldots, k + n_k\}, \tag{1}$$

being

$$n_k = max\{n_{k,1}, \ldots, n_{k,N_{EV}}\} \tag{2}$$

that is the last interval of the time horizon Ω_k that has to be considered when the procedure is applied to the kth time control interval.

Due to the presence of constraints referring to different time intervals, the OP involved in the desired control strategy is multi-period and solved for all the time intervals of Ω_k at the same time.

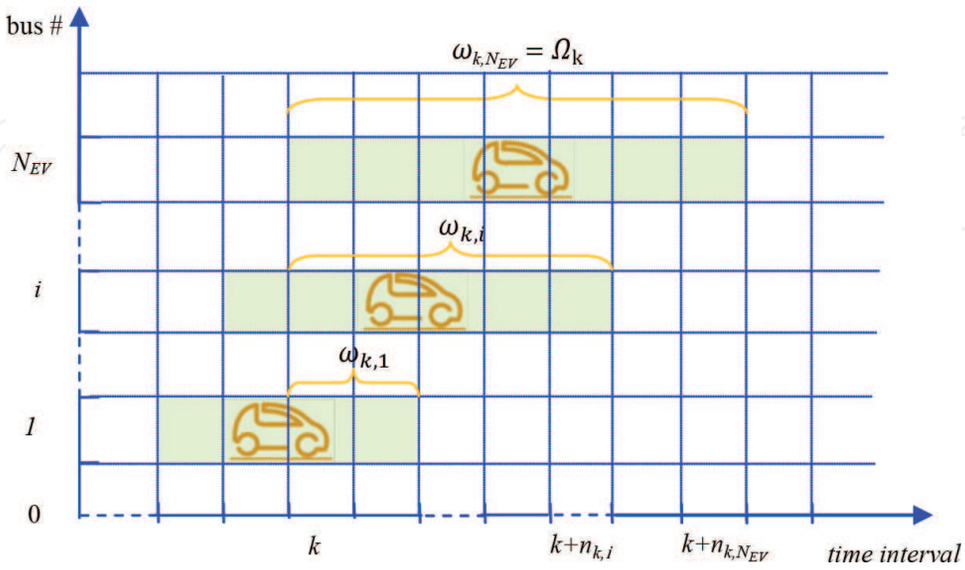

Figure 1. Time horizon of the procedure at the kth control interval.

http://dx.doi.org/10.5772/intechopen.68894

The OP is a single-objective (SO) OP that uses as inputs the values, for all of the time intervals included in Ω_k, of (i) forecasted load demand, (ii) forecasted DG production, and for all of the vehicles that are plugged in at the time interval k, (iii) initial state of charge (SOC) of the on-board batteries, (iv) departure time, and (v) desired value of SOC at the departure time.

Regarding the outputs of the solution of the OP, they are control actions and/or data useful for the monitoring of μG operation. More in detail, in the case of control action, the outputs of the procedure are reference signals that the CCS sends to the interfacing converters of the distributed resources that are the active and reactive phase powers that the EVC exchange with the grid when the vehicles are plugged in, and the reactive phase power requested to the DG units. Outputs useful for the monitoring are (i) the voltage profile at each bus, (ii) the unbalance factor at each bus, and (iii) the currents flowing in the lines. The active power exchanged with the upstream grid at the Point of Common Coupling (PCC) is another output of the procedure that is useful for the knowledge of the μG's energy request and the corresponding cost. **Figure 2** shows a schematic of the proposed control strategy evidencing its inputs and outputs.

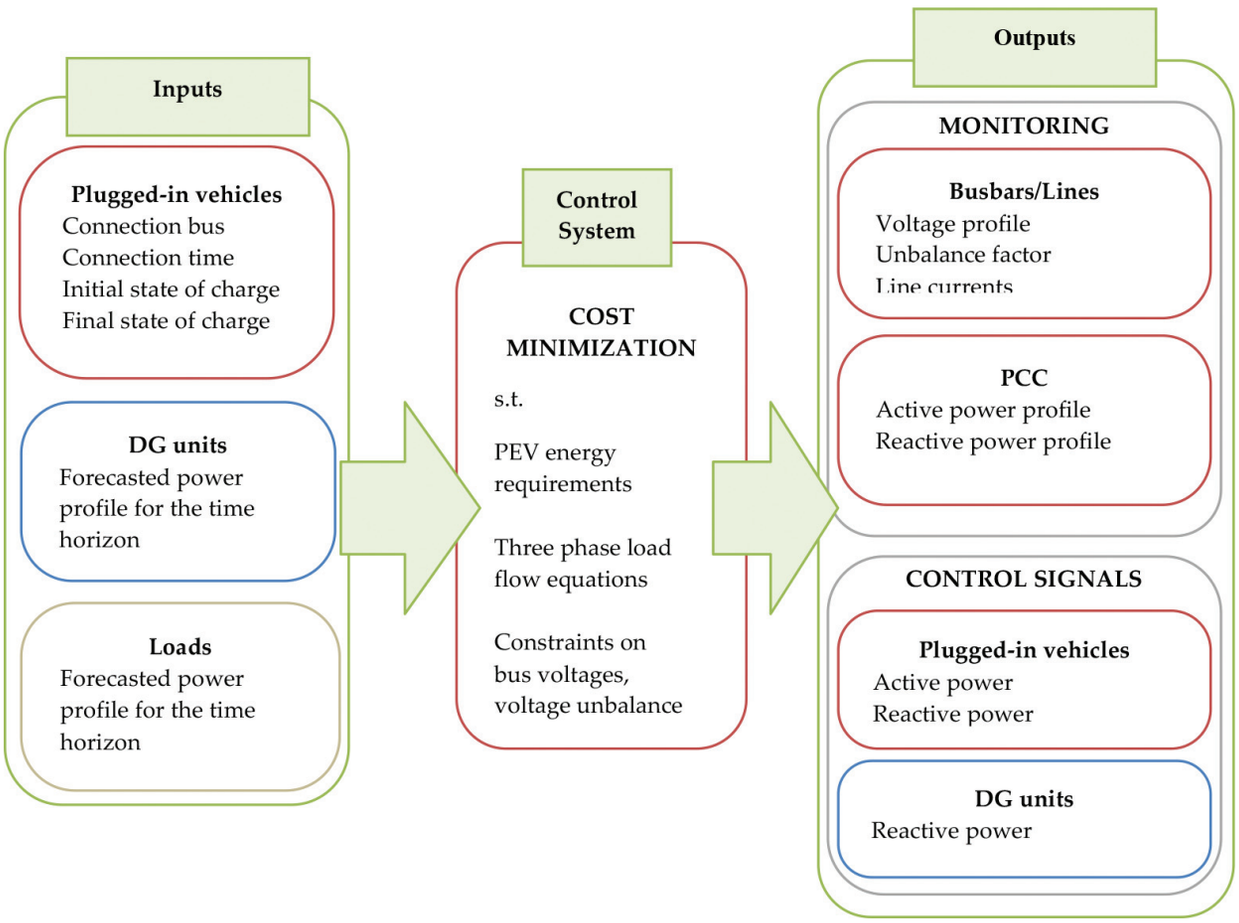

Figure 2. Schematic of the proposed control strategy.

The OP to be solved is formulated as:

$$min\ F(\boldsymbol{x}) \tag{3}$$

subject to:

$$\Psi_h(\boldsymbol{x}) = 0, \quad h = 1,\ldots, n_{eq} \tag{4}$$

$$\eta_m(\boldsymbol{x}) \leq 0, \quad m = 1,\ldots, n_{in} \tag{5}$$

where Ψ_h is the hth equality constraint, η_m is the mth inequality constraint, $\boldsymbol{x}$ is the vector of the optimization variables, $F(\boldsymbol{x})$ is the objective function.

The objective function refers to the cost of the energy purchased from the upstream grid, that is:

$$CE_k = \sum_{\tau \in \Omega_k} \sigma_\tau (P^1_{1,\tau} + P^2_{1,\tau} + P^3_{1,\tau}) \Delta t \tag{6}$$

where $P^1_{1,\tau}$, $P^2_{1,\tau}$, and $P^3_{1,\tau}$ are the phase active powers imported from the upstream grid at the τth time interval and σ_τ is the price of energy during the τth time interval. Regarding this last, a real-time tariff is considered whose variation is on an hourly basis. It has to be noted that, in this formulation, it is assumed that the μG is not allowed to sell energy to the upstream grid.

The equality and inequality constraints can be classified on the basis of the part of the system they refer to. Thus, they are grouped into constraints imposed on:

i. the whole μG;

ii. the slack bus;

iii. the busses where loads are connected;

iv. the busses where DG units are connected, and

v. the busses where plug-in vehicles are connected.

For the sake of clarity, in what follows, busses are supposed to be pure load or pure generation or EVC busses; it is trivial to derive the case of mixed typologies.

3.1. Constraints on the whole μG

Since we deal with unbalanced μGs, the three-phase grid, loads, and generations systems were modeled in phase coordinates [41, 42], and then the three-phase load flow equations are included in the optimization model:

$$P^p_{i,\tau} = V^p_{i,\tau} \sum_{j=1}^{ng} \sum_{q=1}^{3} V^q_{j,\tau} [G^{pq}_{ij} \cos(\vartheta^p_{i,\tau} - \vartheta^q_{j,\tau}) + B^{pq}_{ij} \sin(\vartheta^p_{i,\tau} - \vartheta^q_{j,\tau})] \tag{7}$$

$$\begin{aligned} Q^p_{i,\tau} = V^p_{i,\tau} \sum_{j=1}^{ng} \sum_{q=1}^{3} V^q_{j,\tau} [G^{pq}_{ij} \sin(\vartheta^p_{i,\tau} - \vartheta^q_{j,\tau}) - B^{pq}_{ij} \cos(\vartheta^p_{i,\tau} - \vartheta^q_{j,\tau})], \\ \tau \in \Omega_k, i \in \Omega_G, p = 1, 2, 3 \end{aligned} \tag{8}$$

where ng is the number of μG busses, B_{ij}^{pq} and G_{ij}^{pq} are the terms of the susceptance matrix and of the conductance matrix, respectively, corresponding to the bus i with phase p and the bus j with phase q; $V_{i,\tau}^{p}$ ($V_{j,\tau}^{q}$) is the magnitude of the ith (jth) bus voltage with phase p (q) during the τth time interval; $\vartheta_{i,\tau}^{p}$ ($\vartheta_{j,\tau}^{q}$) is the phase-voltage argument of the ith (jth) bus voltage with phase p (q) during the τth time interval; $P_{i,\tau}^{p}$ and $Q_{i,\tau}^{p}$ are the active and reactive powers injected at the phase p of the ith bus during the τth time interval; Ω_G is the set of μG busses.

Inequality constraints are imposed on the phase-voltage magnitudes that must be within admissible ranges and on the unbalance factor at all busbars that cannot exceed a maximum value:

$$V_{min} \le V_{i,\tau}^{p} \le V_{max}, \quad \tau \in \Omega_k,\ i \in \Omega_G,\ p = 1,2,3 \tag{9}$$

$$kd_{i,\tau} \le kd_{max}, \quad \tau \in \Omega_k,\ i \in \Omega_G \tag{10}$$

where V_{min} and V_{max} are minimum and maximum values for voltage magnitudes, $kd_{i,\tau}$ is the unbalance factor at the ith bus during the τth time interval and kd_{max} is the maximum value imposed to the unbalance factor. The unbalance factor is given by the ratio of the positive and negative components of voltages that are expressed as functions of the bus phase voltages.

The line phase currents cannot exceed the lines' ampacities:

$$I_{l,\tau} \le I_l^r, \quad \tau \in \Omega_k, l \in \Omega_l \tag{11}$$

where $I_{l,\tau}$ is the phase current flowing through line l during the τth time interval expressed as function of bus voltages, I_l^r is the ampacity of the line l, and Ω_l is the set of the μG lines.

3.2. Constraints on the slack bus

Constraints (ii) refer to the magnitude and phase of the voltage at the slack bus ($V_{1,\tau}^{p}$), ($\vartheta_{1,\tau}^{p}$) and on the apparent three-phase power $(P_{1,\tau}{}^2 + Q_{1,\tau}{}^2)^{1/2}$ that can be exchanged with the upstream grid and that must be within the size of the interconnecting transformer (S_{tr}):

$$V_{1,\tau}^{p} = V^{slack}, \quad \tau \in \Omega_k,\ p = 1,2,3 \tag{12}$$

$$\vartheta_{1,\tau}^{p} = \frac{2}{3}\pi(1-p), \quad \tau \in \Omega_k,\ p = 1,2,3 \tag{13}$$

$$(P_{1,\tau}{}^2 + Q_{1,\tau}{}^2)^{1/2} \le S_{tr}, \quad \tau \in \Omega_k \tag{14}$$

with V^{slack} the specified value of the voltage magnitude at slack bus, $P_{1,\tau}$ and $Q_{1,\tau}$ are the three-phase active and reactive powers at the slack bus expressed as functions of the active and reactive phase powers.

3.3. Constraints on the load busses

They refer to the load busses (whose set is Ω_L) where active and reactive powers are equal to specified values ($P_{i,\tau}^{p,sp}$ and $Q_{i,\tau}^{p,sp}$):

$$P_{i,\tau}^{p} = P_{i,\tau}^{p,sp}, \qquad \tau \in \Omega_k, \quad i \in \Omega_L, \quad p = 1,2,3 \tag{15}$$

$$Q_{i,\tau}^{p} = Q_{i,\tau}^{p,sp}, \qquad \tau \in \Omega_k, \quad i \in \Omega_L, \quad p = 1,2,3 \tag{16}$$

3.4. Constraints on DG busses

They refer to the active power ($P_{i,\tau}^{\xi_i}$) at the ith bus DG busses (whose set is Ω_{DG}) with phase ξ_i that must be equal to a specified value ($P_{i,\tau}^{\xi,sp}$) and to the maximum DG unit's apparent power that is constrained by the rating of the interfacing converter at the ith bus with phase ξ_i ($S_{DG,i}^{\xi_i}$):

$$P_{i,\tau}^{\xi_i} = P_{i,\tau}^{\xi_i,sp}, \qquad \tau \in \Omega_k, \quad i \in \Omega_{DG}, \tag{17}$$

$$(P_{i,\tau}^{\xi_i,sp^2} + Q_{i,\tau}^{\xi_i 2})^{\frac{1}{2}} \le S_{DG,i}^{\xi_i}, \qquad \tau \in \Omega_k, \qquad i \in \Omega_{DG} \tag{18}$$

Since we deal with single-phase DG units, the active and reactive powers at the other phases are imposed equal to zero.

3.5. Constraints on EVC busses

Finally, constraints on the EVC bus refer to the limits on the active power at ith bus with the specified phase ξ_i during the τth time interval ($P_{i,\tau}^{\xi_i}$) that is limited by the maximum power that the EVC can absorb from ($P_{EVC_{i,\tau}}^{\xi_i,ch}$) or supply to ($P_{EVC_{i,\tau}}^{\xi_i,dch}$):

$$-P_{EVC_{i,\tau}}^{\xi_i,ch} \le P_{i,\tau}^{\xi_i} \le P_{EVC_{i,\tau}}^{\xi_i,dch}, \qquad \tau \in \omega_{k,i}, \qquad i \in \Omega_{EVk} \tag{19}$$

with Ω_{EVk} the set of nodes where the vehicles are plugged in at the time interval k and $\omega_{k,i}$ the set of time intervals within Ω_k in which the vehicle at the ith bus is connected (see **Figure 1**). Obviously, when the ith vehicle is not connected to the grid, its active power ($P_{i,\tau}^{\xi_i}$) and reactive powers ($Q_{i,\tau}^{\xi_i}$) must be equal to zero:

$$P_{i,\tau}^{\xi_i} = 0, \qquad \tau \notin \omega_{k,i}, \quad i \in \Omega_{EVk} \tag{20}$$

$$Q_{i,\tau}^{\xi_i} = 0, \qquad \tau \notin \omega_{k,i}, \quad i \in \Omega_{EVk} \tag{21}$$

Again, the apparent power at the ith bus, phase ξ_i, must be limited by rating of the charging equipment ($SE_{EVC,i}^{\xi_i}$):

$$(P_{i,\tau}^{\xi_i\ 2} + Q_{i,\tau}^{\xi_i\ 2})^{\frac{1}{2}} \le SE_{EVC,i}^{\xi_i}, \qquad \tau \in \omega_{k,i}, \quad i \in \Omega_{EVk} \tag{22}$$

Finally, constraints on the SOC of the on-board batteries impose that it is limited by the size of the battery ($SE_i^{\xi_i,max}$) and by a minimum value corresponding to the admissible depth of discharge ($SE_i^{\xi_i,min}$):

$$SE_{i,k}^{\xi_i,0} - \sum_{m=k}^{\tau}(\delta_{i,m}^{\xi_i} P_{i,m}^{\xi_i} \Delta t) \le SE_i^{\xi_i,\max}, \qquad \tau \in \omega_{k,i}, \quad i \in \Omega_{EVk} \tag{23}$$

$$SE_{i,k}^{\xi_i,0} - \sum_{m=k}^{\tau}(\delta_{i,m}^{\xi_i} P_{i,m}^{\xi_i} \Delta t) \ge SE_i^{\xi_i,\min}, \qquad \tau \in \omega_{k,i}, \quad i \in \Omega_{EVk} \tag{24}$$

where $SE_{i,k}^{\xi_i,0}$ is the initial value of the energy stored in the battery on board the PEV plugged into the EVC connected to the ith bus with phase ξ_i, and where

$$\delta_{i,m}^{\xi_i} = \begin{cases} \dfrac{1}{\eta_{EVC}} & \text{if } P_{i,m}^{\xi_i} > 0 \\ \eta_{EVC} & \text{if } P_{i,m}^{\xi_i} \le 0 \end{cases} \tag{25}$$

with η_{EVC} the charging efficiency related to the EVC. A specified SOC value is also imposed to the vehicle's battery at the time of departure:

$$SE_{i,k}^{\xi_i,0} - \sum_{m=k}^{k+n_k}(\delta_{i,m}^{\xi_i} P_{i,m}^{\xi_i} \Delta t) = SE_i^{\xi_i,\exp}, \qquad \tau \in \omega_{k,i}, \quad i \in \Omega_{EVk} \tag{26}$$

where, $SE_i^{\xi_i,\exp}$ is the specified value of the energy stored in the battery of the PEV plugged-into the EVC connected to the ith bus with phase ξ_i, at the departure time.

4. Numerical applications

In this section, some results of numerical applications of the proposed control strategy are reported. The test μG considered in this application is the three-phase unbalanced μG reported in **Figure 3**, whose lines' parameters are reported in **Tables 1** and **2**.

The μG is connected to the upstream medium voltage (MV) distribution network through a 250 kVA, 20/0.4 kV transformer. Both single-phase and three-phase loads are connected to the

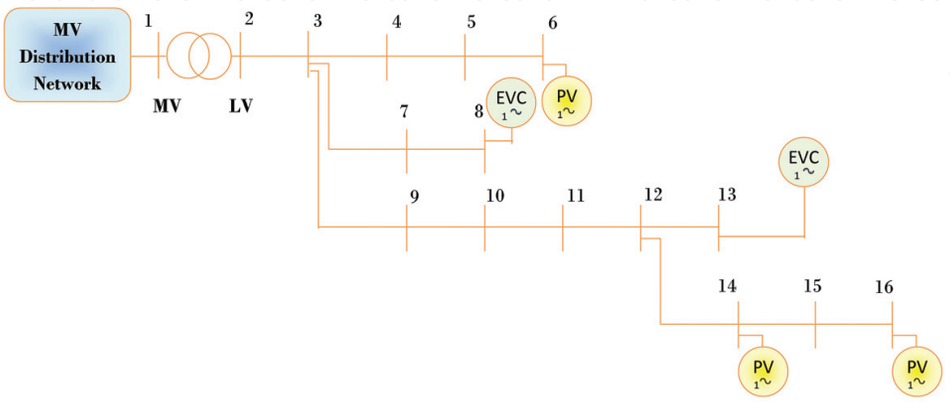

Figure 3. Test network.

Bus		Type	Length [m]	Bus		Type	Length [m]
From	To			From	To		
2	3	T1	100	9	10	T2	81
3	4	T2	137	10	11	T2	70
4	5	T2	168	11	12	T2	93
5	6	T2	10	12	13	T4	174
3	7	T4	107	12	14	T4	66
7	8	T4	102	14	15	T4	86
3	9	T3	162	15	16	T4	173

Table 1. Network data.

Type	Material	$n \times mm^2$	Diam. [mm]	Ampacity [A]
T1	Copper	3×150+95N	53	311
T2	Copper	4×25	28.3	112
T3	Aluminium	3×70+54.6N	37	180
T4	Copper	4×16	24	85

Table 2. Line type.

μG: their nominal active values are reported in **Table 3** ($cos\ \phi$= 0.9 is assumed for all of the loads).

In **Table 3**, bus locations and rated active powers of the photovoltaic systems connected to the μG and of the EVCs are also reported. In this application, it is assumed that all the considered DG units are able to control their reactive power according to the control signals that are outputs of the proposed strategy performed by the μG operator. The rated power values of the converters interfacing DG units correspond to the rated powers of the DG units.

PEVs can be connected to different busses of the μG through EVCs. As an example, the numerical application was performed with reference to the case of two PEVs connected to the μG according to the locations and time schedule of **Figure 4**. The batteries on board the PEVs are assumed to have capacities of 24 kWh; it is assumed that the full SOC is requested at their departure time. The charging (discharging) efficiency is 90% (93%).

With reference to the case of **Figure 4**, the control strategy was applied at each elementary time interval (Δt = 10 min) of the following two time horizons:

- T_1: one PEV is connected to bus i = 13 with phase p = 1: it corresponds to the plugged-in time of the first PEV (from 6:20 to 8:40 a.m.);
- T_2: two PEVs are connected to the μG; the first is connected to bus i = 13 with phase p = 1 (from 8:00 to 8:40 a.m.) and the second is connected to bus i = 8, phase p = 2 (from 8:00 to 11:00 a.m.): it corresponds to the plugged-in time of the PEV connected at 8:00 a.m.

Type	Bus #	Phase	Active power [kW]	Type	Bus #	Phase	Active power [kW]
PV	6	1	5	Load	7	2	6
PV	14	2	5	Load	7	3	3
PV	16	3	5	Load	8	1	3
EVC	8	2	7.4	Load	8	2	3
EVC	13	1	7.4	Load	8	3	3
Load	4	1,2,3	12	Load	13	1	6
Load	10	1,2,3	12	Load	13	2	3
Load	5	1	3	Load	13	3	3
Load	5	2	3	Load	14	1	3
Load	5	3	6	Load	14	2	3
Load	6	1	9	Load	14	3	3
Load	6	2	3	Load	16	1	3
Load	6	3	3	Load	16	2	6
Load	7	1	3	Load	16	3	6

Table 3. Allocation nodes and rated power of loads and DG.

The energy tariff used in this application is an actual real-time tariff [43] whose values in the two considered time horizons are reported in **Figure 5**. This price is assumed to be known 24 h ahead. Loads and DG units' active powers are derived by short-term forecasting procedures. **Figure 6** shows the active power injected at bus $i = 6$ (phase $p = 1$) where both the load and the PV unit are connected. In the figure, two forecasted profiles are shown: the first forecast (**Figure 6a**) refers to all of the intervals of T_1 and is known one time interval ahead the first interval of T_1; the second forecast (**Figure 6b**) refers to all of the intervals of T_2 and is known one time interval ahead the first interval of ahead the first interval of T_2.

Figures 7 and **8** show the active and reactive power profiles of the PEVs connected in the two considered time frames. They are outputs of the procedure and correspond to control signals for the EVCs. **Figure 9** shows the energy stored by the PEVs during the two time horizons.

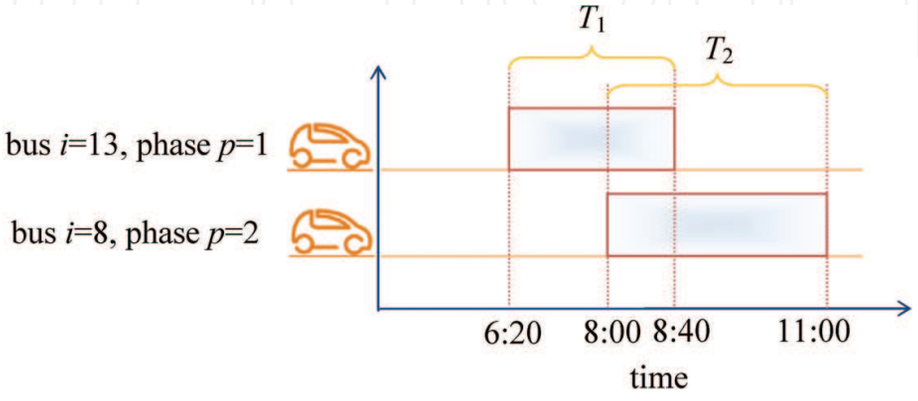

Figure 4. Case study: plug-in time of two plug-in electric vehicles (PEVs).

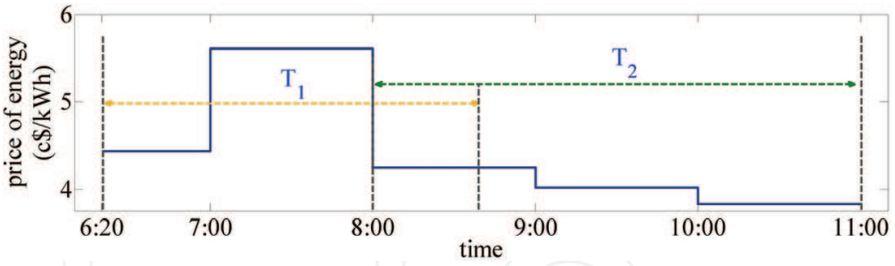

Figure 5. Price of energy.

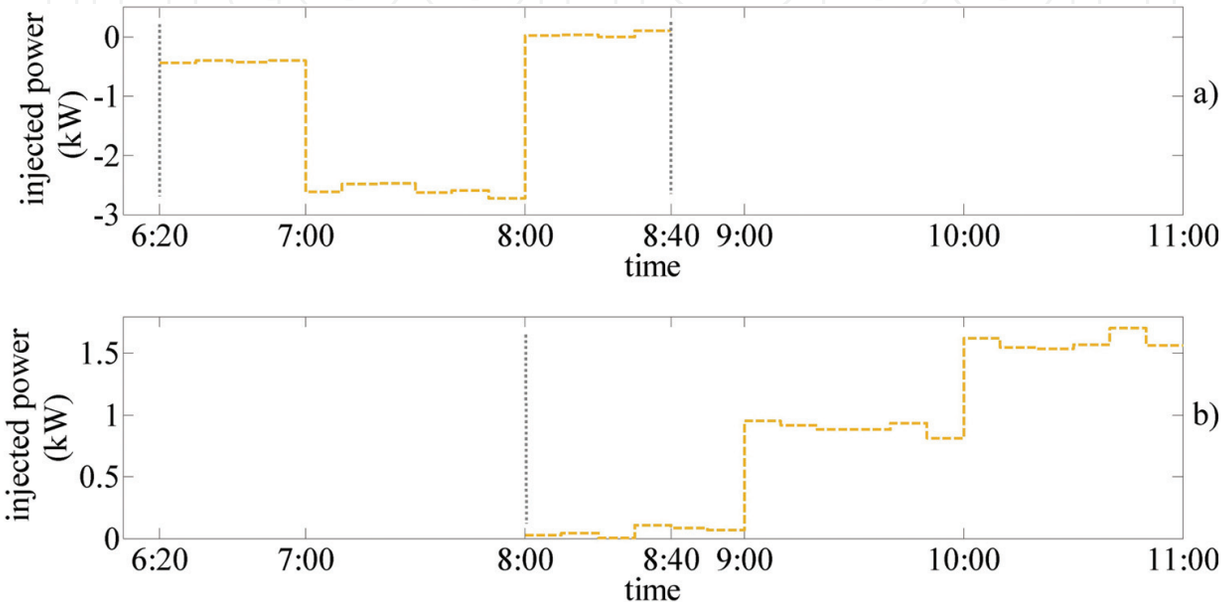

Figure 6. Forecasted value of the injected active power at bus $i = 6$ (phase $p = 1$).

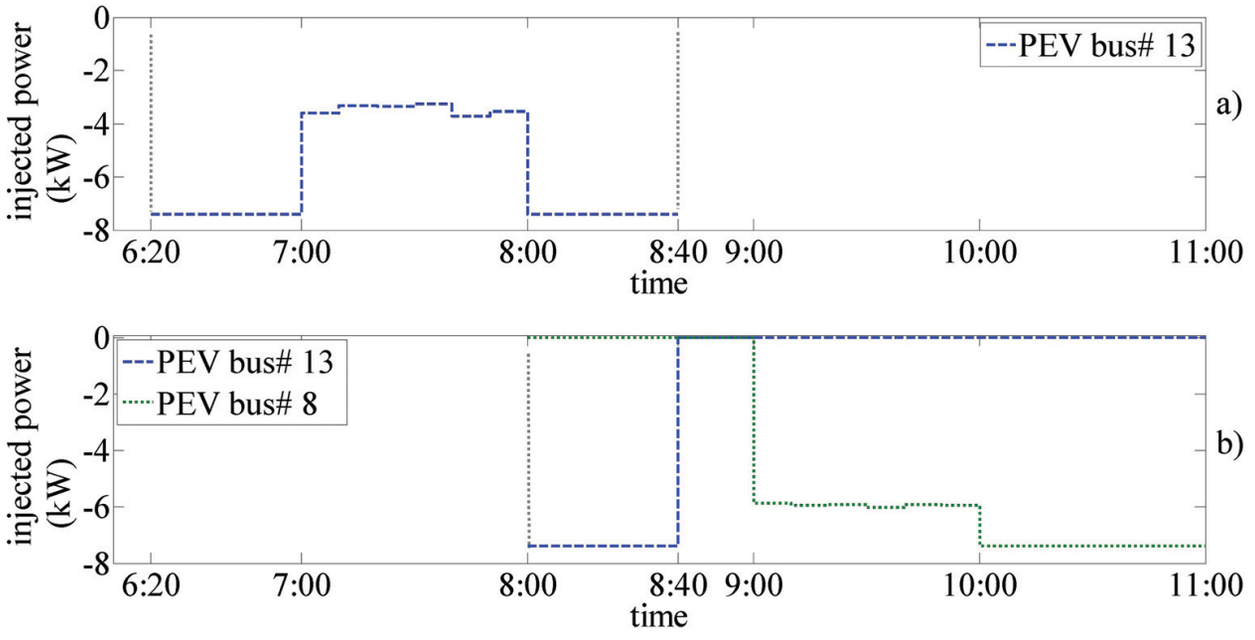

Figure 7. Active power of the PEVs.

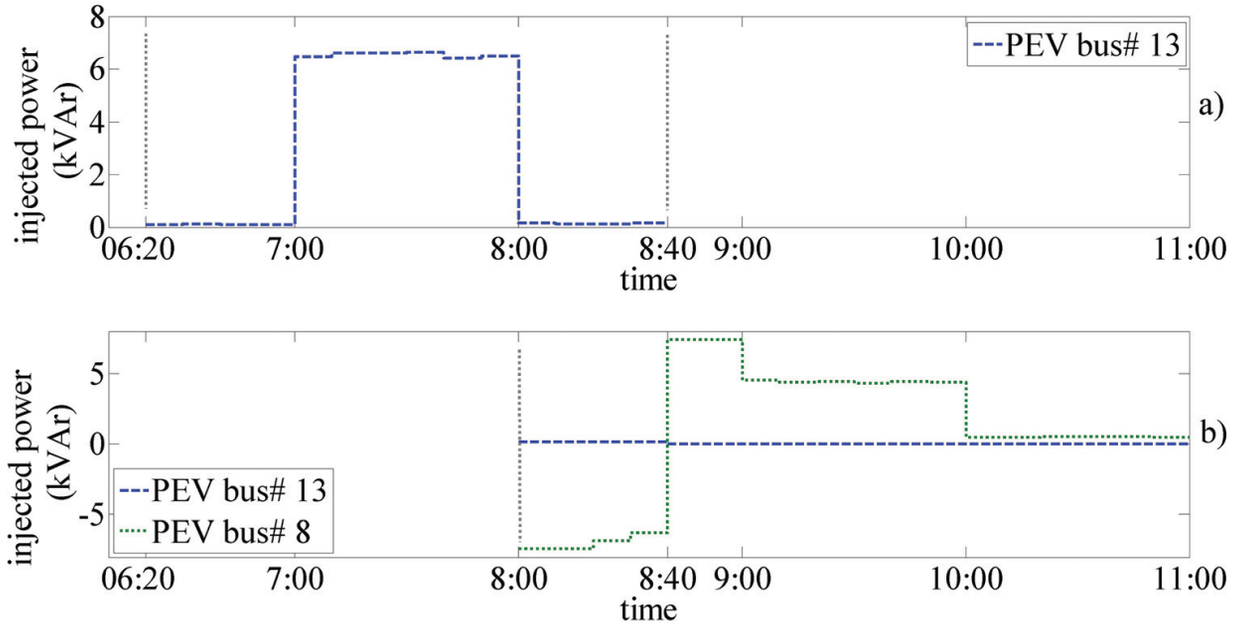

Figure 8. Reactive power of the PEVs during T_1 (a) and T_2 (b).

By the analysis of **Figure 7a**, it clearly appears that in T_1 the EVC reduces its charging in the time interval from 7:00 to 8:00 a.m., that is, the time interval characterized by a higher value of the energy price. In this time interval, the EVC's reactive power increases, in order to reduce both losses and the power requested at the PCC, thus reducing the overall cost for the energy supply sustained by the μG. The same consideration applies to the case of **Figure 7b**. Due to the shortness of the PEV connection time, it can also be noted that the EVCs never discharge.

Figure 10 shows the active power imported at the PCC during T_1 and T_2 in both the uncontrolled and controlled cases. The uncontrolled case corresponds to PEVs charged at the maximum EVC's rated power until the full charge is reached and neither the DG units nor the EVCs provide reactive power support. The figure shows that in the time interval characterized

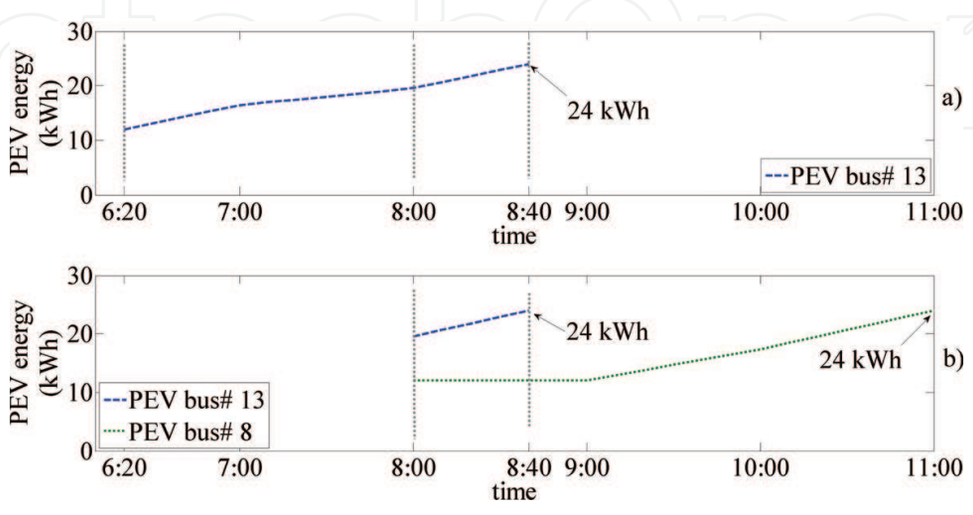

Figure 9. Stored energy of the PEVs during T_1 (a) and T_2 (b).

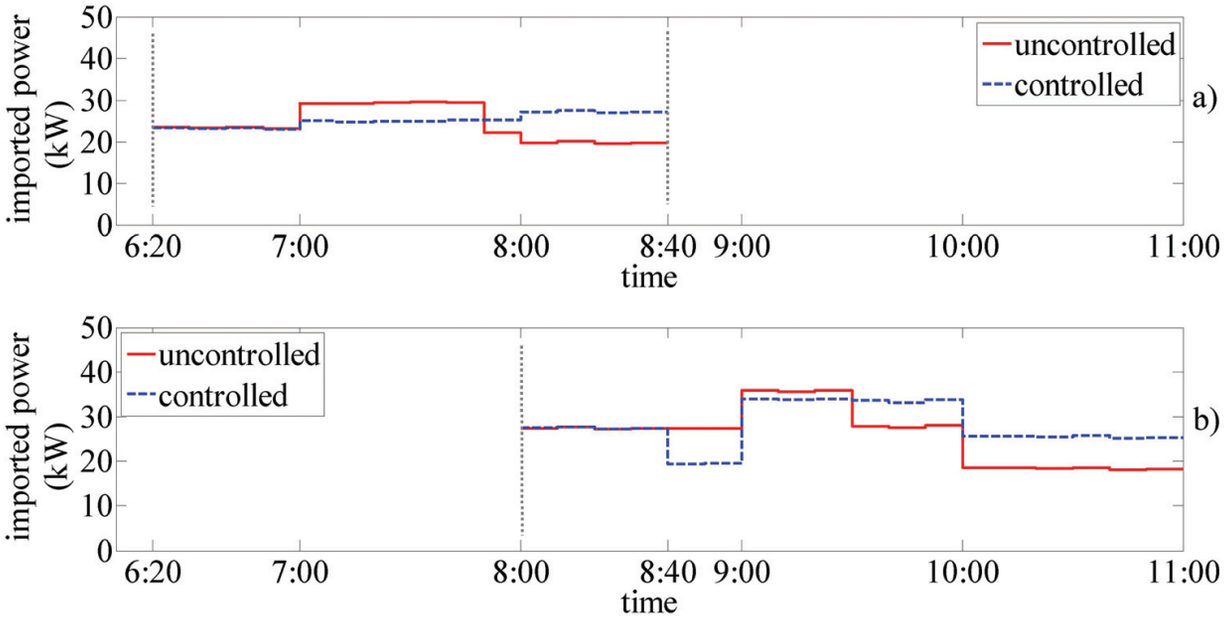

Figure 10. Active power imported at the PCC during T_1 (a) and T_2 (b).

by higher energy price (i.e., 7:00–8:00 a.m.), the energy imported at the PCC in the uncontrolled case is higher than that imported in the controlled case.

Finally, **Figures 11** and **12** show the voltage profile and the voltage unbalance factor, both at the first time interval of T_1.

Figure 11 demonstrates that the bus voltages are always within the limits imposed by regulations (i.e., 0.9–1.1 p.u.). **Figure 12** shows that, in the controlled case, the unbalance factor is

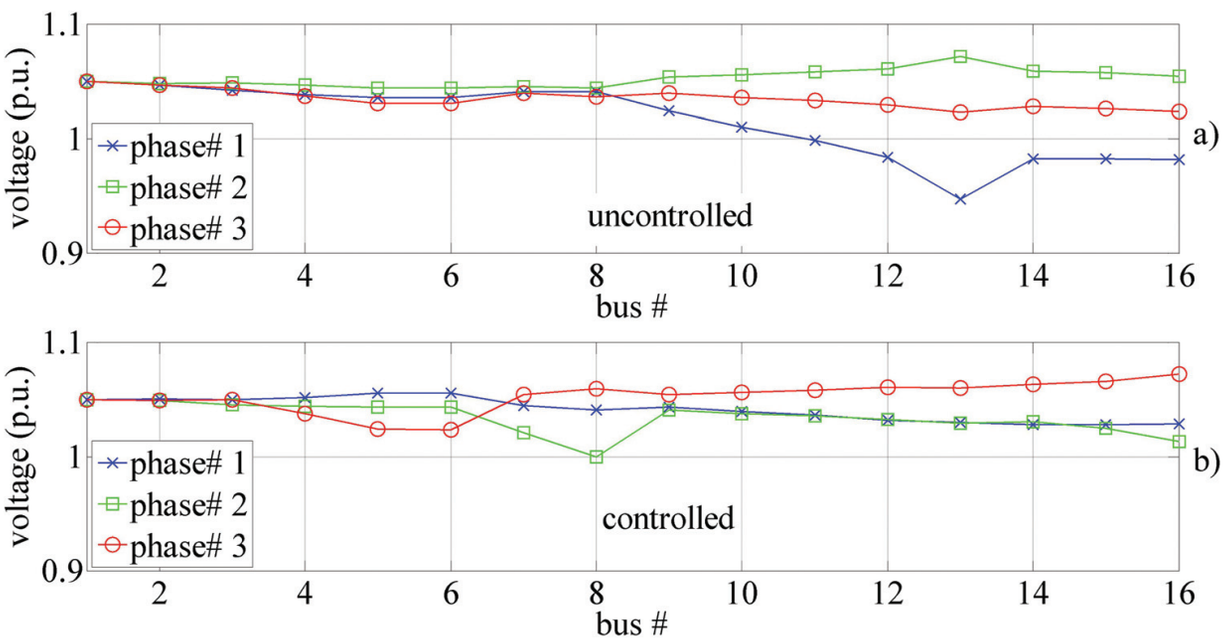

Figure 11. Voltage profile at the first time interval of T_1 in the uncontrolled case (a) and in the controlled case (b).

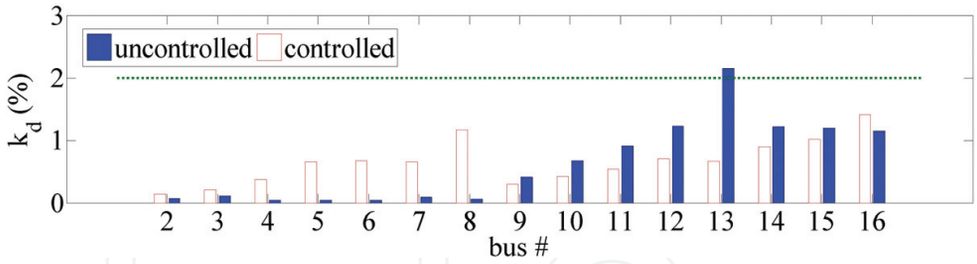

Figure 12. Voltage unbalance factor at the first time interval of T_1.

always lower than the limit of 2%. The proposed control strategy is able to satisfy the requirements in terms of unbalance limits even in particularly critical cases such as the case of bus i = 13, when in the uncontrolled case, the unbalance factor limit is exceeded. In this case, the use of reactive power provided by the DG units (here not reported for the sake of conciseness) and the PEVs is able to reduce the unbalances.

5. Conclusions

In this chapter, an optimal operation strategy was proposed that allowed managing the charging/discharging patterns of the plug-in vehicles connected to an unbalanced LV μG. Aim of the proposed procedure was the minimization of the costs sustained by the μG for the energy provision. The operating strategy allowed complying also with the standard limits for voltage unbalances and slow voltage variations.

Author details

Guido Carpinelli[1]*, Fabio Mottola[1], Daniela Proto[1] and Angela Russo[2]

*Address all correspondence to: guido.carpinelli@unina.it

1 University of Naples Federico II, Naples, Italy

2 Politecnico di Torino, Torino, Italy

References

[1] Kong PY, Karagiannidis GK. Charging schemes for plug-in hybrid electric vehicles in smart grid: A survey. IEEE Access. 2016;**4**:6846–6875

[2] Badtke-Berkow M, Centore M, Mohlin K, Spiller B. Making the Most of Time-Variant Electricity Pricing. Environmental Defense Fund Report; 2015

[3] Carpinelli G, Mottola F, Proto D, Varilone P. Minimizing unbalances in low-voltage microgrids: Optimal scheduling of distributed resources. Applied Energy. 2017;**191**:170–182

[4] Alam MJE, Muttaqi KM, Sutanto D. Alleviation of neutral-to-ground potential rise under unbalanced allocation of rooftop PV using distributed energy storage. IEEE Transactions on Sustainable Energy. 2015;**6**(3):889–898

[5] Li YW, Vilathgamuwa DM, Loh PC. Microgrid power quality enhancement using a three-phase four-wire grid-interfacing compensator. IEEE Transactions on Industry Applications. 2005;**41**(6):1707–1719

[6] Oe SP, Christopher E, Sumner M, Pholboon S, Johnson M, Norman SA. Microgrid Unbalance Compensator: Mitigating the Negative Effects of Unbalanced Microgrid Operation. Lyngby: IEEE/PES Innovative Smart Grid Technologies Europe; 2013

[7] Std EN 50160, Voltage characteristics in public distribution systems; 1999

[8] Gallardo-Lozano J, Milanés-Montero MI, Guerrero-Martínez MA, Romero-Cadaval E. Electric vehicle battery charger for smart grids. Electric Power Systems Research. 2012;**90**:18–29

[9] Hu J, Morais H, Sousa T, Lind M. Electric vehicle fleet management in smart grids: A review of services, optimization and control aspects. Renewable and Sustainable Energy Reviews. 2016;**56**:1207–1226

[10] Richardson DB. Electric vehicles and the electric grid: A review of modeling approaches, impacts, and renewable energy integration. Renewable and Sustainable Energy Reviews. 2013;**19**:247–254

[11] García-Villalobos J, Zamora I, San Martín JI, Asensio FJ, Aperribay V. Plug-in electric vehicles in electric distribution networks: A review of smart charging approaches. Renewable and Sustainable Energy Reviews. 2014;**38**:717–731

[12] Yong JY, Ramachandaramurthy VK, Tan KM, Mithulananthan N. A review on the state-of-the-art technologies of electric vehicle, its impacts and prospects. Renewable and Sustainable Energy Reviews. 2015;**49**:365–385

[13] Shareef H, Islam M, Mohamed A. A review of the stage-of-the-art charging technologies, placement methodologies, and impacts of electric vehicles. Renewable and Sustainable Energy Reviews. 2016;**64**:403–420

[14] Sharma I, Cañizares C, Bhattacharya K. Smart charging of PEVs penetrating into residential distribution systems. IEEE Transactions on Smart Grid. 2014;**5**(3):1196–1209

[15] Martinenas S, Knezović K, Marinelli M. "Management of Power Quality Issues in Low Voltage Networks Using Electric Vehicles: Experimental Validation," in IEEE Transactions on Power Delivery, vol. 32, no. 2, pp. 971–979, April 2017

[16] Kempton W, Letendre SE. Electric vehicles as a new power source for electric utilities. Transportation Research Part D: Transport and Environment. 1997;**2**(3):157–175

[17] Tomić J, Kempton W. Vehicle-to-grid power implementation: From stabilizing the grid to supporting large-scale renewable energy. Journal of Power Sources. 2005;**144**:280–294

[18] Habib S, Kamran M, Rashid U. Impact analysis of vehicle-to-grid technology and charging strategies of electric vehicles on distribution networks: A review. Journal of Power Sources. 2015;**277**(1):205–214

[19] Rabiee A, Feshki Farahani H, Khalili M, Aghaei J, Muttaqi KM. Integration of plug-in electric vehicles into microgrids as energy and reactive power providers in market environment. IEEE Transactions on Industrial Informatics. 2016;**12**(4):1312–1320

[20] Tomić J, Kempton W. Using fleets of electric-drive vehicles for grid support. Journal of Power Sources. 2007;**168**(2):459–468

[21] Peças Lopes JA, Polenz SA, Moreira CL, Cherkaoui R. Identification of control and management strategies for LV unbalanced microgrids with plugged-in electric vehicles. Electric Power Systems Research. 2010;**80**(8):898–906

[22] Wu T, Yang Q, Bao Z, Yan W. Coordinated energy dispatching in microgrid with wind power generation and plug-in electric vehicles. IEEE Transactions on Smart Grid. 2013;**4**(3):1453–1463

[23] Su W, Wang J, Roh J. Stochastic energy scheduling in microgrids with intermittent renewable energy resources. IEEE Transactions on Smart Grid. 2014;**5**(4):1876–1883

[24] Honarmand M, Zakariazadeh A, Jadid S. Integrated scheduling of renewable generation and electric vehicles parking lot in a smart microgrid. Energy Conversion and Management. 2014;**86**:745–755

[25] Zhang M, Chen J. The energy management and optimized operation of electric vehicles based on microgrid. IEEE Transactions on Power Delivery. 2014;**29**(3):1427–1435

[26] Guo Y, Xiong J, Xu S, Su W. Two-stage economic operation of microgrid-like electric vehicle parking deck. IEEE Transactions on Smart Grid. 2016;**7**(3):1703–1712

[27] Rabiee A, Sadeghi M, Aghaeic J, Heidari A. Optimal operation of microgrids through simultaneous scheduling of electrical vehicles and responsive loads considering wind and PV units uncertainties. Renewable and Sustainable Energy Reviews. 2016;**57**:721–739

[28] Mortaz E, Valenzuela J. Microgrid energy scheduling using storage from electric vehicles. Electric Power Systems Research. 2017;**143**:554–562

[29] Tabatabaee S, Mortazavi SS, Niknam T. Stochastic scheduling of local distribution systems considering high penetration of plug-in electric vehicles and renewable energy sources. Energy. 2017;**121**:480–490

[30] Kou P, Liang D, Gao L, Gao F. Stochastic coordination of plug-in electric vehicles and wind turbines in microgrid: A model predictive control approach. IEEE Transactions on Smart Grid. 2016;**7**(3):1537–1551

[31] Yang H, Pan H, Luo F, Qiu J, Deng Y, Lai M, Dong ZY. "Operational Planning of Electric Vehicles for Balancing Wind Power and Load Fluctuations in a Microgrid," in IEEE Transactions on Sustainable Energy, vol. 8, no. 2, pp. 592–604, April 2017.

[32] Tushar M, Assi C, Maier M, Uddin M. Smart microgrids: Optimal joint scheduling for electric vehicles and home appliances. IEEE Transactions on Smart Grid. 2014;**5**(1):239–250

[33] Van Roy J, Leemput N, Geth F, Büscher J, Salenbien R, Driesen J. Electric vehicle charging in an office building microgrid with distributed energy resources. IEEE Transactions on Sustainable Energy. 2014;**5**(4):1389–1396

[34] Beer S, Gómez T, Dallinger D, Marnay C, Stadler M, Lai J. An economic analysis of used electric vehicle batteries integrated into commercial building microgrids. 2012;**3**(1):517–525

[35] Deckmyn C, Van de Vyver J, Vandoorn TL, Meersman B, Desmet J, Vandevelde L. Day-ahead unit commitment model for microgrids. IET Generation, Transmission & Distribution. 2017;**11**(1):1–9

[36] Tafreshi S, Ranjbarzadeh H, Jafari M, Khayyam H. A probabilistic unit commitment model for optimal operation of plug-in electric vehicles in microgrid. Renewable and Sustainable Energy Reviews. 2016;**66**:934–947

[37] López MA, Martín S, Aguado JA, de la Torre S. V2G strategies for congestion management in microgrids with high penetration of electric vehicles. Electric Power Systems Research. 2013;**104**:28–34

[38] Gouveia C, Moreira CL, Lopes JAP, Varajao D, Araujo RE. Microgrid service restoration: The role of plugged-in electric vehicles. IEEE Industrial Electronics Magazine. 2013;**7**(4):26–41

[39] Khooban MH, Niknam T, Blaabjerg F, Dragičević T. A new load frequency control strategy for micro-grids with considering electrical vehicles. Electric Power Systems Research. 2017;**143**:585–598

[40] Rana R, Singh M, Mishra S. Design of modified droop controller for frequency support in microgrid using fleet of electric vehicles. IEEE Transactions on Power Systems; in press, IEEE Early Access Article (doi: 10.1109/TPWRS.2017.2651906)

[41] Arrillaga J, Arnold CP. Computer Analysis of Power System. John Wiley & Sons; Chichester, West Sussex, England; 1990

[42] Laughton MA. Analysis of unbalanced polyphase networks by the method of phase coordinates. Part 1: System representation in phase frame of reference. IEE Proceedings. 1968;**115**(8):1163–1172

[43] Comed Residential Real-Time Pricing Program [Internet]. Available from: https://rrtp.comed.com/live-prices/?date=20150318